Biophysical Journal
Article

Biophysical Society

An Asymmetry in Monolayer Tension Regulates Lipid Droplet Budding Direction

Aymeric Chorlay[1] and Abdou Rachid Thiam[1,*]
[1]Laboratoire de Physique Statistique, Ecole Normale Supérieure, PSL Research University, Sorbonne Université, UPMC Université Paris 06, Université Paris Diderot, CNRS, Paris, France

ABSTRACT Cells store excess energy in the form of neutral lipids that are synthesized and encapsulated within the endoplasmic reticulum intermonolayer space. The lipids next demix to form lipid droplets (LDs), which, surprisingly, bud off mostly toward the cytosol. This directional LD formation is critical to energy metabolism, but its mechanism remains poorly understood. Here, we reconstituted the LD formation topology by embedding artificial LDs into the intermonolayer space of bilayer vesicles. We provide experimental evidence that the droplet behavior in the membrane is recapitulated by the physics of three-phase wetting systems, dictated by the equilibrium of surface tensions. We thereupon determined that slight tension asymmetries between the membrane monolayers regulate the droplet budding side. A differential regulation of lipid or protein composition around a forming LD can generate a monolayer tension asymmetry that will determine the LD budding side. Our results offer, to our knowledge, new insights on how the proteins might regulate LD formation side by generating a monolayer tension asymmetry.

INTRODUCTION

Biological membranes are made up of two adhering phospholipid monolayers that form a bilayer. The properties of this bilayer are crucial for various biological mechanisms and rely strongly on bilayer lipid composition. This is illustrated by the difference in membrane composition between cellular organelles (1), which perform different tasks. For example, as compared to other organelle membranes, the plasma membrane is enriched in lipid surfactants such as cholesterol or specific charged phospholipids (2). The endoplasmic reticulum (ER) membrane can instead particularly contain neutral lipids, which are oily molecules, or fat, localized at the interstice between the two monolayers composing the membrane (3) (Fig. 1 *A*). This happens typically in energy-rich conditions under which neutral lipids such as triglycerides, sterol or retinyl esters, or squalene are produced by enzymes directly inside the ER intermonolayer membrane (4). These lipids can affect the ER membrane properties, disrupt it, and mediate protein unfolding and ER stress (5,6). However, at a certain concentration, the neutral lipids probably demix, forming a lipid lens within the bilayer (Fig. 1 *A*), which further grows by accumulating lipids (7,8). In cells, this phenomenon presumably drives the removal of neutral lipids from the ER bilayer, packaging them into organelles called oil bodies or lipid droplets (LDs) (9).

LDs are oil droplets covered by a phospholipid monolayer containing proteins; they constitute a newly identified class of organelles whose formation and regulation are critical for cellular energy metabolism (10,11). LDs bud off from the ER bilayer membrane and, remarkably, mainly toward the cytosol (12,13). The mechanisms responsible for the packaging of neutral lipids into droplets and LD directional budding are still weakly understood. However, LDs can be seen as the disperse phase of an intracellular oil-in-water emulsion (7,14), and therefore, LD formation can be considered as an emulsification mechanism of oil-in-water droplets from the ER bilayer. Soft-matter physics, which describes such typical phenomena, should thus enable a better comprehension of the mechanism of LD directional formation (7). We decided to take advantage of such knowledge to identify the biophysical parameters governing LD directional formation and shed light on how proteins might regulate cytosolic LD biogenesis (15).

Studying the biophysics of LD budding requires knowledge of the behavior of oil molecules in a bilayer. It is now possible to acquire such knowledge by various in vitro model systems based on giant unilamellar vesicles (GUVs) made in the presence of oils. This is the case, for example, when GUVs are prepared using

Submitted September 26, 2017, and accepted for publication December 11, 2017.

*Correspondence: thiam@lps.ens.fr

Editor: Markus Deserno.
https://doi.org/10.1016/j.bpj.2017.12.014

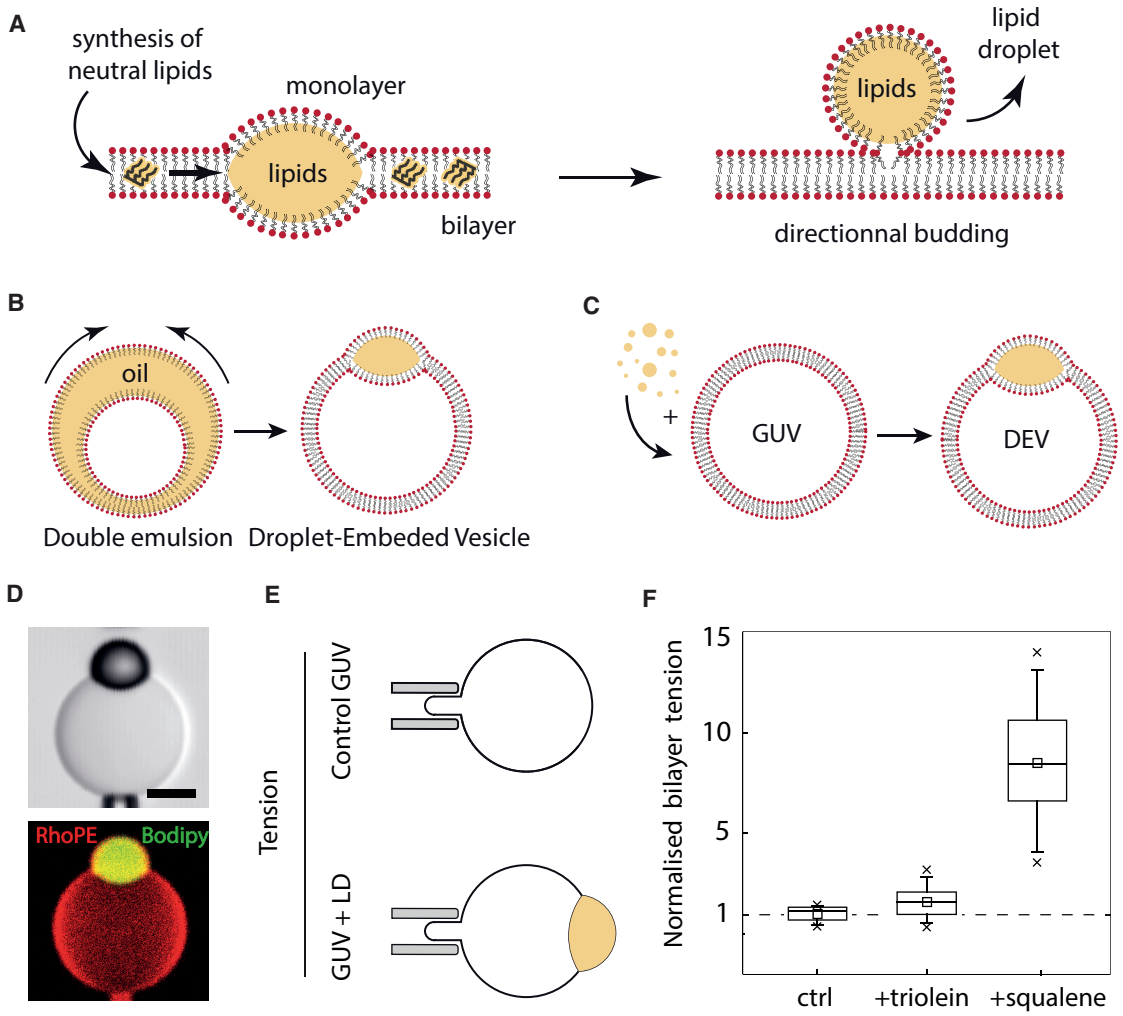

FIGURE 1 The presence of neutral lipids increases bilayer surface tension. (*A*) Schematic description of LD formation steps. (*B*) The oil film of a water-in-oil-in-water double emulsion (made by microfluidics, see (14) for more detail) spontaneously collapses to form a GUV embedded with an LD. (*C*) GUVs are mixed with artificial LDs that are incorporated into the intermonolayer space of the GUVs to form a GUV embedded with an LD, termed DEVs. (*D*) Reconstitution of an artificial LD (Bodipy stained) embedded in the intermonolayer space of a PC (dioleoylphosphatidylcholine) GUV using the technique described in (*B*). Rhodamine-PE (0.5% w/w to PC) is used to visualize the membranes by fluorescence. Scale bars, 10 μm. (*E*) Microaspiration is used to measure bilayer tension of a GUV in the presence and absence of an LD. Micrographs of the experiments are shown in Fig. S1. (*F*) Bilayer tensions of a different set of GUVs normalized by the average GUV tension without an LD (3.10–2 mN/m): control and embedded LDs of triolein and squalene. $N = 10$, 9, and 11, respectively. To see this figure in color, go online.

water-in-oil-in-water double emulsions (Fig. 1 *B*) or inverted emulsion methods (16,17). In these situations, a large oil film is first generated between two monolayers before it collapses into an oil droplet (Fig. 1 *B*). The resulting system is a vesicle embedded with an LD. Recently, we have developed an alternative system in which we first make GUVs by electroformation and afterward incorporate oil droplets directly within the intermonolayer space (18,19) (Fig. 1 *C*)—we term this system droplet-embedded vesicles (DEVs). DEVs offer minimal systems mimicking the topology of an LD forming in the ER bilayer; their surface tensions or membrane physical chemistry can be finely modulated to isolate relevant parameters controlling LD directional budding.

We hypothesized that the DEV topology is a three-phase system in which the equilibrium between surface tensions dictates droplet shape (20,21). We here bring the tensions into play and show that, regardless of the physical chemistry of the membrane, their equilibrium indeed follows a three-phase wetting theory, i.e., the shape of a droplet, described by the angle it forms with the bilayer, is dictated by the balance of surface tensions (7). We suggest that the budding of the model LDs corresponds to a full dewetting situation, i.e., generation of a spherical droplet sharing a neck with the bilayer (Fig. 1 *A*). The exclusive formation of droplets on one side of the membrane requires keeping an imbalance of surface tensions between the two monolayers enclosing the droplet. Such tension imbalance can arise from a

mechanically imposed difference of tensions between the monolayer leaflets and/or an asymmetry in protein or phospholipid composition dynamically generated by the action of enzymes. Our results thus bring new insights, to our knowledge, on how proteins might act in cells to modulate the formation of cytosolic LDs.

MATERIALS AND METHODS

GUV preparation

Unless stated otherwise, all GUVs were 99.5% 1,2-dioleoyl-*sn*-glycero-3-phosphocholine (DOPC) and 0.5% (w/w) Rhodamine-DOPE. GUVs were prepared by electroformation (19). Phospholipids and mixtures thereof in chloroform at 0.5 μM were dried on an indium-tin-oxide-coated glass plate. The lipid film was desiccated for 1 h. The chamber was sealed with another indium-tin-oxide-coated glass plate. The lipids were then rehydrated with a sucrose solution (275 $\pm$ 15 mOsm). Electroformation is performed using 100 Hz alternating-current voltage at 1.0–1.4 Vpp and maintained for at least 1 h. This low voltage was used to avoid hydrolysis of water and dissolution of the titanium ions on the glass plate. GUVs were either stored in the chamber at 4°C overnight or directly collected with a Pasteur pipette.

Buffer HKM composition

Unless mentioned, experiments were performed in a buffer of 50 mM Hepes, 120 mM Kacetate, and 1 mM MgCl2 (in Milli-Q water) at pH 7.4 and 275 $\pm$ 15 mOsm.

Incorporation of droplets into GUV membranes to make DEVs

To prepare GUVs embedded with artificial LDs, 5 μL of the oil was added to 45 μL of HKM buffer. The mixture was sonicated for 1 min. GUVs were then incubated with the artificial LDs for 5 min under gentle mixing. The GUV-LD mixture was then placed on a glass coverslip, pretreated with 10% (w/w) bovine serum albumin (BSA), and washed three times with buffer.

Micromanipulation and surface tension measurements by micro aspiration

Micropipettes were made from capillaries drawn out with a Sutter Instruments (Novato, CA) pipette puller. They were used to manipulate the LD-embedded GUVs to get a side view of the system. The pipettes were incubated for 30 min in a 5% BSA solution before use, to prevent droplets and membranes from adhering to the glass.

Additionally, surface tensions were measured and modulated using the same pipettes. As shown in (Fig. 1 *D*), the micromanipulation of the external LD monolayer (and bilayer) enables the measurement and modulation of surface tension (γ). Using Laplace's law and the measurement of the pipette inner diameter, droplet diameter, and suction pressure, the surface tension of the interface can be determined (19) as

$$\gamma = \frac{\Delta P\mathrm{suc}}{2\left(\frac{1}{Rp} - \frac{1}{Rd}\right)},$$

where ΔPsuc, Rp, and Rd are the suction pressure, the pipette radius, and the droplet (or GUV) radius.

The suction was carried out using a syringe. The resulting pressure was measured with a pressure transducer (DP103, Validyne Engineering, Northridge, CA), the output voltage of which was monitored with a digital voltmeter. The pressure transducer (range 55 kPa) was calibrated before the experiments were performed.

Reagents

Glyceryl trioleate (triolein) (T7140) and squalene (S3626) were from Sigma Aldrich (St. Louis, MO). Phospholipids used were DOPC, rhodamine-1,2-dioleoyl-*sn*-glycero-3-phosphoethanolamine (rhodamine-DOPE), and lysophosphatidylcholine (LysoPC) (18:1) from Avanti Polar Lipids (Alabaster, AL). Bodipy (D3922, Molecular Probes, Eugene, OR) was used at 1:100 of a 10 mg/mL stock concentration. BSA 98% (A7906-100G) and sucrose 99.5% (59378- 500G) were purchased from Sigma-Aldrich.

Equipment

All micrographs were made on a laser scanning microscope (LSM 800, Carl Zeiss, Oberkochen, Germany). Glass coverslips (24 $\times$ 36 mm #0) were from Menzel Glaser (Braunschweig, Germany). Micropipettes made from capillaries (1.0 OD $\times$ 0.58 ID $\times$ 150 L (mm); 30-0017 GC100-15b, Harvard Apparatus, Holliston, MA) were used with a micropipette puller (model P-2000, Sutter Instruments). Micromanipulation was achieved using TransferMan 4r (Eppendorf, Hamburg, Germany). The pressure measurement unit was provided by Validyne Engineering (DP103).

RESULTS

The presence of neutral lipids increases bilayer surface tension

We generated dioleoylphosphatidylcholine (PC) GUVs of low tension by electroformation and mixed part of them with triolein or squalene (Fig. 1, *C* and *D*), which are biological oils synthesized in different cell types (10). We measured with microaspiration techniques the bilayer tension of each sample and found that GUVs mixed with oil, i.e., forming DEVs, systematically had a significantly higher bilayer surface tension than control GUVs (Fig. 1, *E* and *F*). This is likely due to the localization of oil molecules into the intermonolayer space of the bilayer. The subsequent increase of surface tension probably arises from different contributions. This increase might originate from the higher energy cost of the interaction between the acyl chains of phospholipids and oil molecules, as compared to the interaction between facing phospholipids in a pure bilayer. In addition, the accumulation of oil molecules in the bilayer tends to make the membrane similar to two phospholipid-covered oil-water interfaces, which have higher surface tension (1–30 mN/m (18,19,22)) than pure bilayer membranes (0.001–1 mN/m (23–25)).

We also noted that for the same phospholipid composition, i.e., PC, triolein and squalene differently increased the bilayer tension (Fig. 1 *F*), which probably reflects the difference in affinity of the oils with phospholipids and/or surrounding water phase. Changing the membrane phospholipid composition would also change the relative tension variation (18). In conclusion, our results show that the presence of neutral lipids in a bilayer increases surface tension.

Thus, as compared to classical bilayer organelles, the ER bilayer might acquire higher surface tensions because of the presence of neutral lipids. Packaging neutral lipids into LDs would make it possible to reduce tension, maintain ER membrane integrity, and avoid bilayer stress.

The balance of tensions determines droplet shape in a bilayer

We recently found that decreasing the bilayer tension favors the removal of neutral lipids from the bilayer and their packaging into spherical droplets (18). Here, we experimentally observed that the shape of the droplet indeed depends on the bilayer tension, which was mechanically varied (Fig. 2 *A*). A spherical droplet was obtained at lower bilayer tension; a higher bilayer tension led to a droplet having a lense-like shape. We previously assumed that the droplet shape is determined by the equilibrium between the various tensions (Fig. 2 *B*), as is the case for three-phase wetting situations (20,26). Such equilibrium would yield

$$\gamma_{int}\ \sin(\alpha)\ =\ \gamma_{ext}\ \sin(\theta) \tag{1}$$

and

$$\gamma_b\ =\ -\gamma_{int}\cos(\alpha) - \gamma_{ext}\cos(\theta), \tag{2}$$

where γ represents surface tension and α and θ are the different angles formed between the bilayer and monolayers (Fig. 2 *B*). This assumption is valid only when the membrane bending contribution, given by its bending modulus, κ, can be neglected. This condition is satisfied when the droplet size is $>(\kappa/\gamma)^{1/2} \sim 20$ nm, when taking $\kappa \sim 10 k_B T$ and $\gamma \sim 1$ mN/m, which are typical values for a phospholipid monolayer (18,22,27). The size of cellular LDs is well above 50 nm (28), which implies that surface tensions might be at some level the main physical parameters that determine the formation of spherical LDs.

If the balance of tensions determines the droplet shape, the membrane physical chemistry should not be directly

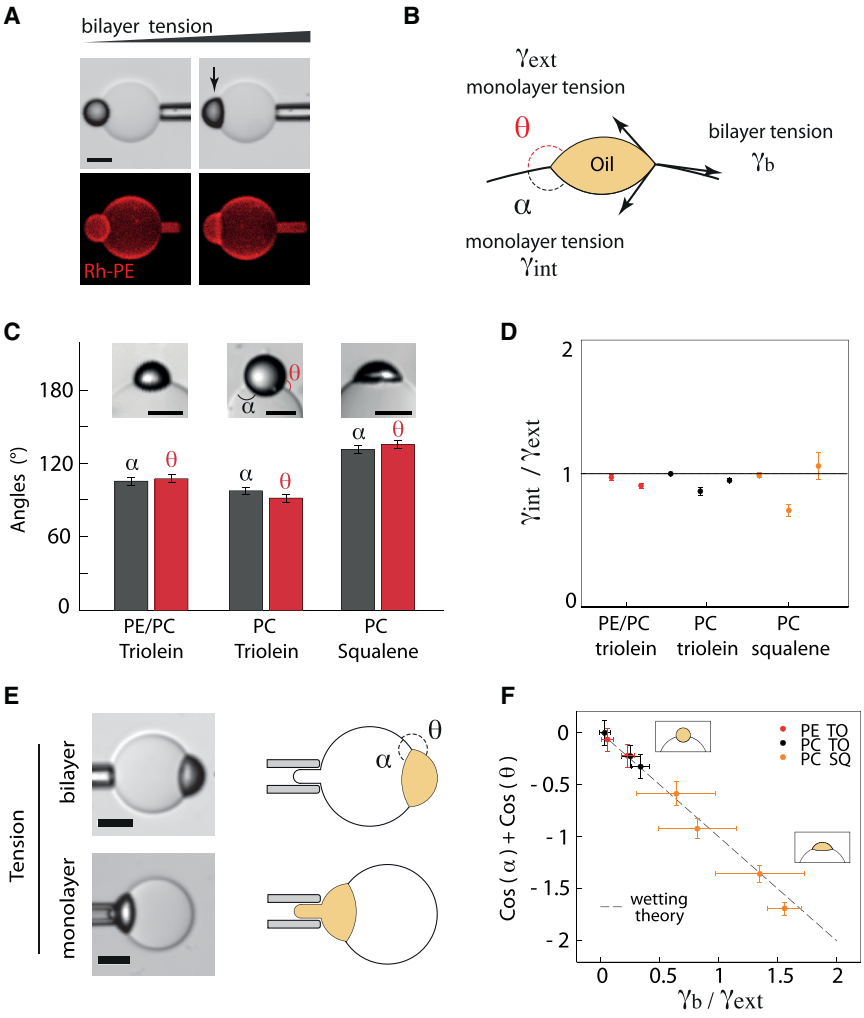

FIGURE 2 The equilibrium of tensions determines droplet shape in a bilayer according to a wetting theory. (*A*) A triolein LD embedded in a PC GUV spreads in the bilayer when tension is increased by the microaspiration technique. Scale bars, 10 μm. (*B*) Illustration of an LD embedded in a bilayer, showing the biophysical parameters controlling its shape: external and internal monolayer tension, and bilayer tension. The two angles α and θ describe the shape and position of the LD. (*C*) Angles α and θ correspond to different oil droplet (triolein or squalene) and membrane compositions (PE/PC 40:60 or PC 100%). Scale bars, 10 μm. (*D*) Ratios of internal to external surface tension corresponding to the angles in (*B*), calculated using the equilibrium-of-tensions law described by Eq. 1. Eight measurements of different physical chemistry conditions were probed with varying phospholipid/oil compositions. (*E*) Method of measurement of the external monolayer and bilayer tensions using micropipettes. The suction by the micropipette is correlated to the surface tension through the Laplace law. (*F*) Experimental α and θ sum of cosine is displayed as a function of the ratio of bilayer to monolayer tensions, corresponding to the experimental conditions in (*D*). The wetting theory prediction from Eq. 3 is displayed as a dashed line. To see this figure in color, go online.

involved. We thus studied different phospholipid and oil compositions. Using electroformation, we made PC/PE and PC GUVs, to vary the membrane composition, and embedded them with triolein oil droplets to make DEVs. We also embedded trioelin and squalene droplets in PC GUVs to change the neutral lipid oil composition instead of phospholipids. We observed that the embedded droplets adopted different shapes (Fig. 2 *C*). For all lipid conditions, however, the droplets were often positioned in the middle of the bilayer, i.e., $\alpha = \theta$ (Fig. 2 *C*). This would imply from Eq. 1 that the inner and outer monolayers of these droplets have the same tension (Fig. 2 *D*), which is plausible, as no asymmetry was introduced during GUV formation. Thus, by assuming that $\gamma_{int} = \gamma_{ext}$, Eq. 2 can be written simply as

$$\gamma_b/\gamma_{ext} = -(\cos(\alpha) + \cos(\theta)). \quad (3)$$

Experimentally, we can measure γ_b and γ_{ext} by micropipette aspiration, and the angles, which are geometrical parameters (Fig. 2 *E*). We observed that all lipid conditions follow Eq. 3 (see Fig. 2 *F*). This result provides evidence that the balance between the monolayer and bilayer tensions exclusively determines the droplet shape in the bilayer.

Modeling the role of surface tensions in droplet shape and budding direction

Considering that the droplet shape is exclusively determined by surface tensions, we developed a basic model (Supporting Material, Text S1) that allowed us to draw a phase diagram describing the behavior of a droplet in a bilayer. The droplet is subjected to two monolayer tensions that pull on the contact line to make it spherical, and to the bilayer tension, which pulls in the opposite direction to flatten it (Fig. 2 *B*). When the bilayer tension is substantially higher than the monolayer tensions, the droplet tends to adopt a lens-like shape (Fig. 3 *A*). In the extreme case, when $\gamma_b - \gamma_{int} - \gamma_{ext} \geq 0$, which can be rewritten as

$$\gamma_{int}/\gamma_{ext} \leq \gamma_b/\gamma_{ext} - 1, \quad (4)$$

oil molecules contained in the droplet are entirely spread in the bilayer (Fig. 3 *A*, *pink region*).

For a given bilayer tension, if the external monolayer surface tension of the droplet is higher than the internal tension, the pressure of the external bulk fluid will push the droplet inside the membrane due to the Laplace effect. If, instead, the inner monolayer surface tension is higher, the luminal pressure will be higher than the bulk pressure and will push the droplet to the outside. In the extreme situations where the droplet fully buds internally or externally, the tensions follow $(\gamma_{ext} - \gamma_{int}) - \gamma_b \geq 0$ and $(\gamma_{int} - \gamma_{ext}) - \gamma_b \geq 0$, respectively, which can be rewritten as

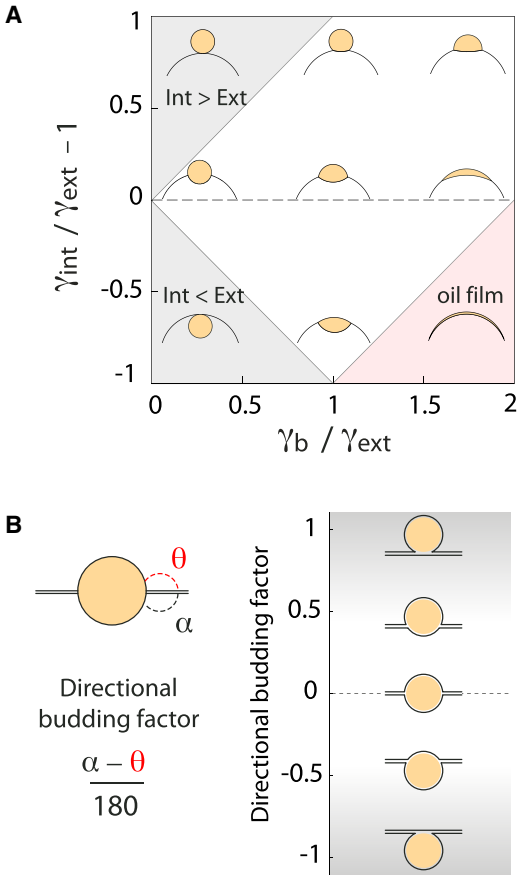

FIGURE 3 Modeling of the role of surface tensions on LD shape and budding direction. (*A*) The competition between the three different surface tensions (bilayer, external monolayer, and internal monolayer tensions) determines LD shape in the bilayer. The phase diagram shows simulated LD shape and position according to the competition between bilayer and external monolayer tensions, and the ratio between external and internal monolayer tensions (see Supporting Material, Text S2). High bilayer tensions flatten the LD and imbalance between internal and external tension dictates the budding direction. The top gray region corresponds to full external budding, low bilayer tensions, and internal tensions larger than external tensions; the bottom gray region corresponds to full internal budding, low bilayer tensions, and internal tensions smaller than external tensions. The pink region corresponds to full spreading of the oil film in the bilayer (unstable condition). (*B*) Directional budding factor describing the position of the LD relative to the bilayer and corresponding LD positions, here displayed at low bilayer tension (spherical LD). To see this figure in color, go online.

$$\gamma_{int}/\gamma_{ext} \leq 1 - \gamma_b/\gamma_{ext} \quad (5)$$

and

$$\gamma_{int}/\gamma_{ext} \geq 1 + \gamma_b/\gamma_{ext}. \quad (6)$$

Equations 4, 5, and 6 delineate the regions of the phase diagram, showing the different shape and budding direction of the droplets (Fig. 3 *A*). This phase diagram was also numerically calculated (unpublished data) using a

mathematical model that takes into account a GUV bilayer containing an LD (Supporting Material, Text S1).

In summary, the diagram recapitulates that the imbalance between the monolayer tensions determines the position of the droplet with respect to the bilayer, and that the droplet is pushed toward the side with the lower monolayer surface tension. The droplet can be fully budded on either the inside of the membrane (Fig. 3 *A*, *lower gray region*) or the outside (Fig. 3 *A*, *upper gray region*), or can remain in the bilayer, with varying degrees of contact with the interior and exterior (Fig. 3 *A*). When the monolayer tensions are equal, the LD lies in the middle of the bilayer, except for very low bilayer tension ($\gamma_b/\gamma_{ext} < \sim 0.2$), for which effective line tensions can theoretically promote the spontaneous budding of the droplet (27) but would not control the budding direction.

An asymmetry in monolayer tension determines LD budding direction

A currently unanswered question regarding the mechanism of LD biogenesis is how LD exclusive formation in the cytosol is achieved. This is an important question for lipid metabolism because lipid fluxes strongly rely on the accessibility of LDs to cytosolic proteins. Our analysis of the role of tensions in LD shape and position suggests that controlling the LD budding side or direction is possible by constantly maintaining a tension asymmetry between the monolayer leaflets (Fig. 3 *A*). Surface tensions are generally controlled mechanically or chemically by the presence of surfactants, which can be lipids or proteins. We probed these predictions in our DEV system.

We prepared PC GUVs and incorporated them with LDs. We used microaspiration to modulate surface tensions in the resulting DEV system. We can modulate and measure both bilayer and external monolayer tensions, separately or concurrently, by pulling on their respective membranes (Fig. 2 *E*). The tension of the inner monolayer can be inferred from the droplet shape (Supporting Material, Text S2).

At the outset, the LDs were centered in the bilayer. To characterize the droplet position, we defined the directional budding factor as the relative angle or position shift of the LD between the inside and outside of the membrane (see Fig. 3 *B*). Initially, the directional budding factor was close to 0 (Fig. 4, *A* and *B*). We increased the outer monolayer tension and observed that the LD was displaced into the GUV lumen (Fig. 4 *A*, *arrow*; Fig. S2 *C arrow*); the directional budding factor was consequently largely negative (Fig. 4 *B*). Measurement of the tension values confirmed that an asymmetry of monolayer tension was maintained (Fig. 4 *C*; Fig. S2, *C–E*). The final set of surface tensions is consistent with the droplet shape predicted by the phase diagram (Fig. S2 *A*). These observations show that physically maintaining a tension asymmetry can enable control over the droplet budding side.

In cells, the surface tension of the cytosolic monolayer of a forming LD can be modulated, for example, by the asymmetrical insertion or action of proteins such as perilipins or complex protein I (19,29). Proteins might also modulate the phospholipid monolayer composition to generate an asymmetry of tension. This is the case of phospholipases, for example, which mainly act on the cytosolic face of LDs.

We probed the effect of the phospholiphase A2 (PLA2), which is involved in cellular LD formation, by transforming phospholipids into lysophospholipids (18,30). We made GUVs containing LDs and added PLA2 enzyme to the external bulk solution (Fig. S4, *A* and *B*), which makes lysophospholipids only on the external monolayer a priori; the conversion of PC to Lyso-PC on GUVs by PLA2 has been proven using thin-layer chromatography in our previous work (18). Over time, we observed dynamic changes of shape and position of the droplet in the bilayer. The droplet moved toward the interior of the GUV, suggesting an increase of the external monolayer tension. This tension increase likely arose from the replacement of PC by Lyso-PC

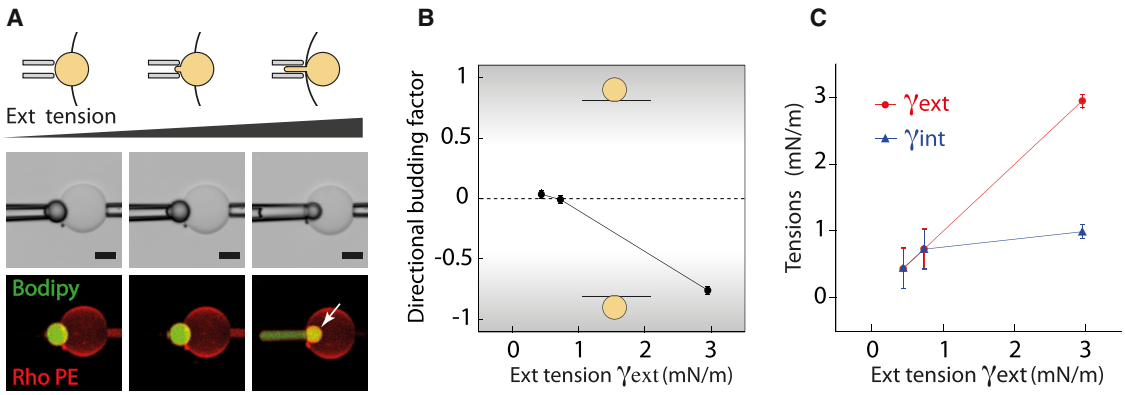

FIGURE 4 Asymmetry between monolayer tensions determines droplet budding direction. (*A*) A triolein LD embedded in a GUV. Increasing the external monolayer tension with a micropipette causes the internalization of the LD. Scale bars, 10 μm. (A similar experiment with a squalene LD and the bilayer tension kept constant is shown in Fig. S2, *C–E*). (*B*) The directional budding factor drastically decreases due to the internalization of the LD. (*C*) Throughout the internalization process, the internal tension remains roughly constant as external tension is increased. To see this figure in color, go online.

in the external monolayer. Substituting PC with Lyso-PC in the monolayer introduces more phospholipid packing defects on the external monolayer, which results in an increase of surface tension. Indeed, a fully packed PC monolayer on a triolein droplet has a tension of ~0.6 mN/m, whereas a pure Lyso-PC monolayer has a higher tension, >2 mN/m (18). It is worth noting that these monolayer tension values are much higher than bilayer tensions, which are usually well below 1 mN/m. Consequently, we think that spontaneous curvatures, which mediate bilayer deformation, would have a smaller impact on the monolayer deformation because of the high monolayer tension values. Our results thus suggest that keeping an asymmetry of phospholipid type around a forming LD gives rise to asymmetric monolayer tensions and might regulate the side of LD budding.

High bilayer tensions repress the effect of tension asymmetry on the droplet budding direction

According to the phase diagram (Fig. 3 *A*), LD directional formation is essentially controlled by an asymmetry in monolayer tension. However, the diagram also suggests that a low bilayer tension is necessary to facilitate the budding step (18,27) by decreasing the required monolayer tension asymmetry (Fig. 3 *A*). Consequently, increasing the bilayer tension should repress budding and, considering the phase diagram, reduce the effect of monolayer tension asymmetry on the droplet directional formation. We experimentally tested this prediction.

We embedded an LD in a GUV bilayer and introduced a slight tension asymmetry by increasing its external tension (see droplet tongue suctioned into the micropipette (Fig. 5 *A*)). This caused the droplet to bulge into the GUV lumen (Fig. 5 *A*, *arrow*). While maintaining the suction on the external monolayer, we pulled on the bilayer to increase its tension (Fig. 5 *A*). This operation repressed the internalization, equilibrated the monolayer tensions, and recentered the droplet in the middle of the bilayer (Fig. 5, *B* and *C*). This observation confirmed that increasing the bilayer tension reduces the asymmetry of monolayer tensions. All together, our results predict that having a higher surface tension on the luminal monolayer of an LD, along with a low ER bilayer tension, will guarantee budding in the cytosol (Fig. 6 *A*). Finely tuning ER molecular composition in the cell can enable the meeting of such requirements.

DISCUSSION

We have experimentally demonstrated that the shape and position in a bilayer of a reconstituted LD are determined by the equilibrium between the tensions of the bilayer and two monolayers enclosing the droplet, as in three-phase wetting systems; this result is valid when droplet size is >20 nm. Our result thus highlights how a cell might exploit well-known physical concepts of wetting processes to exclude fat from membranes and mediate an emulsification process mediating LD formation. Concretely, high bilayer surface tension leads to disperse neutral lipids in the membrane. Decreasing the bilayer tension enables packaging of the neutral lipids into spherical droplets (Figs. 2 *A*, 3 *A*, and 6 *A*) (18,27). The budding direction is determined by the tension asymmetry between the monolayers; budding happens toward the side of lower monolayer tension

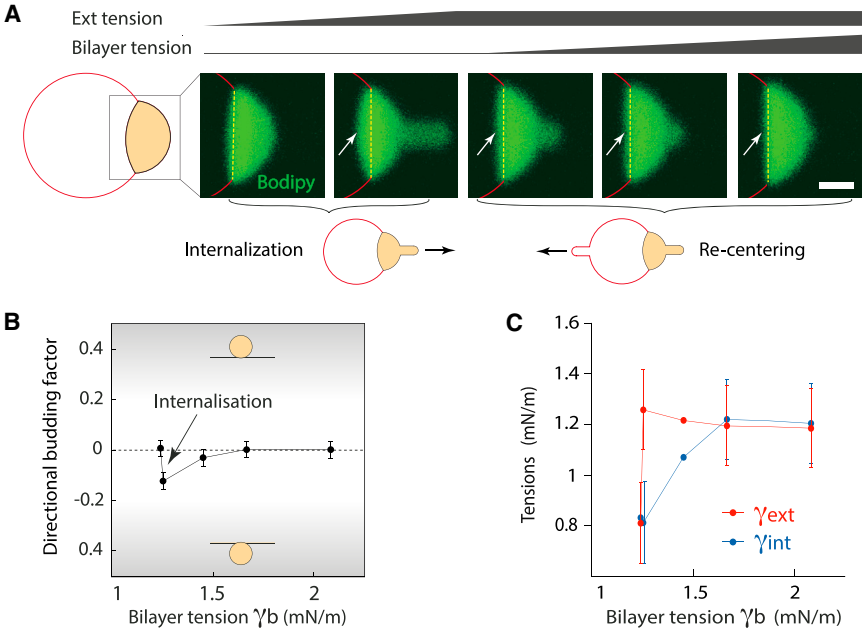

FIGURE 5 High bilayer tensions repress the effect of tension asymmetry on directional budding. (*A*) An artificial LD is slightly internalized by an increase of its external tension. Then, increasing the bilayer tension recenters the LD. Scale bars, 10 μm (full pictures are shown in Fig. S3 *A*). (*B*) Increase of external over internal tension diminishes the directional budding factor. An increase in bilayer tension recenters the LD and thus brings the directional budding factor back to zero. (*C*) Internal and external monolayer tensions are plotted as a function of bilayer tension. The asymmetrization of monolayer tension is suppressed by increasing bilayer tension. These tensions are in part calculated as described in Text S2 in the Supporting Material, with angles displayed in Fig. S3 *B*. To see this figure in color, go online.

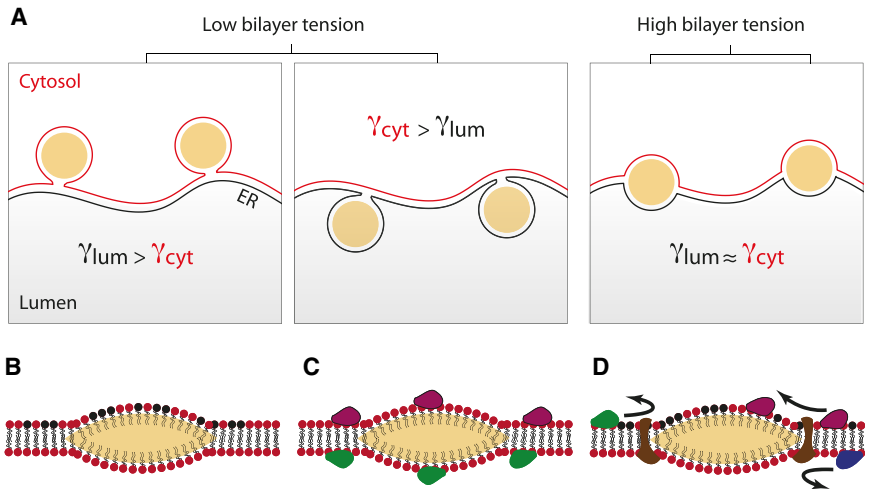

FIGURE 6 Model for the role of surface tensions and excess of phospholipids in LD position and contact with different cell compartments. (*A*) At high bilayer tensions, LDs are centered and spread in the middle of the bilayer. Lowering the tension allows budding of the droplets toward the side with the lower monolayer tension. (*B*) Asymmetry in phospholipid composition between the two sides of the bilayer. (*C*) Asymmetry of protein repartition on the two sides of the bilayer. (*D*) Transmembrane proteins that might regulate the protein and phospholipid asymmetry. To see this figure in color, go online.

(Fig. 6 *A*). These various tensions are very likely modulated in cells to control cytosolic LD formation. For example, altering ER phospholipid composition, and potentially shape, by the action of phospholipid remodeling enzymes and/or shaping proteins, modulates ER bilayer surface tension and LD formation (18,30,31). To guarantee LD exclusive formation in the cytosol, a constant lower tension of the cytosolic over the luminal monolayer should be maintained around forming LDs. Questions to address are how and which proteins modulate tensions of the cytosolic and luminal monolayers to guarantee LD formation toward the cytosol.

Proteins might regulate monolayer surface tensions by different means. A first class of proteins can directly bind LDs from the cytosol, or the ER membrane or its lumen, and generate an asymmetry in monolayer tensions. This can be achieved by locally creating an asymmetry in protein and lipid composition between the monolayer leaflets (Fig. 6, *B* and *C*), as different lipid and protein compositions proffer different monolayer tensions (18,19,22,32). Such action could be mediated by lipid remodeling enzymes such as phospholipases, lipin, or diacylglycerol-acyltransferase (30,33,34). Other proteins binding LDs can physically modulate the monolayer tension (Fig. 6 *C*). In the cytosol, this might be the case for perilipin proteins, or the complex protein I machinery that mechanically deforms the LD surface (19,29). Whether these proteins affect LD budding direction is currently not known.

There is a second class of proteins that do not bind LDs but can affect their budding directionality. These are ER-resident transmembrane proteins encompassing the fat-storage-inducing transmembrane protein 2 and seipin, which are the two main ER-resident proteins so far identified as key regulators of LD formation (35). However, only fat-storage-inducing transmembrane protein 2 has been shown so far to be critical for LD budding directionality (28). These proteins localize at LD-ER junctions or rims and could regulate the surface tensions of the cytosolic and luminal monolayers to generate the required asymmetry. Such asymmetry could be achieved by modulating phospholipids and proteins localizing on both monolayers (Fig. 6 *D*).

The budding of LDs toward the cytosol is critical for cellular metabolism because proteins regulating LDs are mainly present in the cytosol. The degree of contact of LDs with the cytosol will determine to what extent LDs are accessible to cytosolic and ER luminal proteins (36,37). Our results highlight the potential role of tensions in regulating the amount of LD surface accessible to these proteins. Since LDs within a single cell are different, based on their protein content, it is plausible that surface tensions are dynamically modulated to enable the formation of different LDs. This might explain the existence of LD subsets that are more exposed to the ER lumen (37,38). These LDs would potentially be implicated in specific metabolic pathways, such as in the biogenesis of lipoproteins or lipoviral particles (39,40). Indeed, these LDs are more accessible, for example, to the microsomal triglyceride transfer protein, which needs to access triglycerides for the biogenesis of apolipoprotein B (36,37,40). Our results suggest that these LD subsets would have a particularly high surface tension on their cytosolic leaflet, caused, for example, by the action of proteins such as complex protein I (19,29,41).

In conclusion, our findings suggest that the cytosolic LD biogenesis mechanism might simply arise from a phase-separation mechanism described by three-phase wetting systems. The physics of such systems is well documented. Establishing it in the context of LD formation enables us to make good projections on the role of proteins in regulating the direction of LD formation. We thereby bring important insights into the mechanisms of cytosolic LD formation and accessibility to

proteins and pave the way for a better understanding of LD function and mechanisms of lipid secretion. Reaching such a level of comprehension will have major implications for the diagnosis and treatment of metabolic disorders.

SUPPORTING MATERIAL

Supporting Materials and Methods and six figures are available at http://www.biophysj.org/biophysj/supplemental/S0006-3495(17)35094-4.

AUTHOR CONTRIBUTIONS

A.R.T. conceived the project and A.C. conducted experimental work. A.C. and A.R.T. analyzed data. A.R.T. wrote the manuscript with feedback from A.C.

ACKNOWLEDGMENTS

We thank Drs. Lionel Forêt and Kalthoum Ben M'barek for their critical reading of the manuscript and helpful discussions. We also thank all the members of the group for comments and critical discussions, especially Kamran Ramji for editing the manuscript.

This work was supported by the ATIP-Avenir program, the Programme Emergence de la Ville de Paris, a Paris Sciences et Lettres installation grant, and NANODROP project supported by the ANR to A.R.T. The EDPIF program supports A.C.

REFERENCES

1. van Meer, G., D. R. Voelker, and G. W. Feigenson. 2008. Membrane lipids: where they are and how they behave. *Nat. Rev. Mol. Cell Biol.* 9:112–124.
2. van Meer, G., and A. I. de Kroon. 2011. Lipid map of the mammalian cell. *J. Cell Sci.* 124:5–8.
3. Murphy, D. J., and J. Vance. 1999. Mechanisms of lipid-body formation. *Trends Biochem. Sci.* 24:109–115.
4. Buhman, K. K., H. C. Chen, and R. V. Farese, Jr. 2001. The enzymes of neutral lipid synthesis. *J. Biol. Chem.* 276:40369–40372.
5. Holthuis, J. C., and A. K. Menon. 2014. Lipid landscapes and pipelines in membrane homeostasis. *Nature.* 510:48–57.
6. Volmer, R., and D. Ron. 2015. Lipid-dependent regulation of the unfolded protein response. *Curr. Opin. Cell Biol.* 33:67–73.
7. Thiam, A. R., and L. Forêt. 2016. The physics of lipid droplet nucleation, growth and budding. *Biochim. Biophys. Acta.* 1861 (8 Pt A):715–722.
8. Pol, A., S. P. Gross, and R. G. Parton. 2014. Review: biogenesis of the multifunctional lipid droplet: lipids, proteins, and sites. *J. Cell Biol.* 204:635–646.
9. Martin, S., and R. G. Parton. 2006. Lipid droplets: a unified view of a dynamic organelle. *Nat. Rev. Mol. Cell Biol.* 7:373–378.
10. Walther, T. C., and R. V. Farese, Jr. 2012. Lipid droplets and cellular lipid metabolism. *Annu. Rev. Biochem.* 81:687–714.
11. Fujimoto, T., Y. Ohsaki, …, Y. Shinohara. 2008. Lipid droplets: a classic organelle with new outfits. *Histochem. Cell Biol.* 130:263–279.
12. Ohsaki, Y., M. Suzuki, and T. Fujimoto. 2014. Open questions in lipid droplet biology. *Chem. Biol.* 21:86–96.
13. Ohsaki, Y., J. Cheng, …, T. Fujimoto. 2009. Biogenesis of cytoplasmic lipid droplets: from the lipid ester globule in the membrane to the visible structure. *Biochim. Biophys. Acta.* 1791:399–407.
14. Thiam, A. R., R. V. Farese, Jr., and T. C. Walther. 2013. The biophysics and cell biology of lipid droplets. *Nat. Rev. Mol. Cell Biol.* 14:775–786.
15. Joshi, A. S., H. Zhang, and W. A. Prinz. 2017. Organelle biogenesis in the endoplasmic reticulum. *Nat. Cell Biol.* 19:876–882.
16. Arriaga, L. R., S. S. Datta, …, D. A. Weitz. 2014. Ultrathin shell double emulsion templated giant unilamellar lipid vesicles with controlled microdomain formation. *Small.* 10:950–956.
17. Pautot, S., B. J. Frisken, and D. Weitz. 2003. Production of unilamellar vesicles using an inverted emulsion. *Langmuir.* 19:2870–2879.
18. Ben M'barek, K., D. Ajjaji, …, A. R. Thiam. 2017. ER membrane phospholipids and surface tension control cellular lipid droplet formation. *Dev. Cell.* 41:591–604.e7.
19. Thiam, A. R., B. Antonny, …, F. Pincet. 2013. COPI buds 60-nm lipid droplets from reconstituted water-phospholipid-triacylglyceride interfaces, suggesting a tension clamp function. *Proc. Natl. Acad. Sci. USA.* 110:13244–13249.
20. Kusumaatmaja, H., and R. Lipowsky. 2011. Droplet-induced budding transitions of membranes. *Soft Matter.* 7:6914–6919.
21. Roux, A., and R. Loewith. 2017. Tensing up for lipid droplet formation. *Dev. Cell.* 41:571–572.
22. Thiam, A. R., and F. Pincet. 2015. The energy of COPI for budding membranes. *PLoS One.* 10:e0133757.
23. Morris, C. E., and U. Homann. 2001. Cell surface area regulation and membrane tension. *J. Membr. Biol.* 179:79–102.
24. Upadhyaya, A., and M. P. Sheetz. 2004. Tension in tubulovesicular networks of Golgi and endoplasmic reticulum membranes. *Biophys. J.* 86:2923–2928.
25. Shi, Z., and T. Baumgart. 2015. Membrane tension and peripheral protein density mediate membrane shape transitions. *Nat. Commun.* 6:5974.
26. Neeson, M. J., R. F. Tabor, …, D. Y. Chan. 2012. Compound sessile drops. *Soft Matter.* 8:11042–11050.
27. Deslandes, F., A. R. Thiam, and L. Forêt. 2017. Lipid droplets can spontaneously bud off from a symmetric bilayer. *Biophys. J.* 113:15–18.
28. Choudhary, V., N. Ojha, …, W. A. Prinz. 2015. A conserved family of proteins facilitates nascent lipid droplet budding from the ER. *J. Cell Biol.* 211:261–271.
29. Wilfling, F., A. R. Thiam, …, T. C. Walther. 2014. Arf1/COPI machinery acts directly on lipid droplets and enables their connection to the ER for protein targeting. *Elife.* 3:e01607.
30. Gubern, A., J. Casas, …, E. Claro. 2008. Group IVA phospholipase A2 is necessary for the biogenesis of lipid droplets. *J. Biol. Chem.* 283:27369–27382.
31. Klemm, R. W., J. P. Norton, …, H. Y. Mak. 2013. A conserved role for atlastin GTPases in regulating lipid droplet size. *Cell Reports.* 3:1465–1475.
32. Small, D. M., L. Wang, and M. A. Mitsche. 2009. The adsorption of biological peptides and proteins at the oil/water interface. A potentially important but largely unexplored field. *J. Lipid Res.* 50 (*Suppl*):S329–S334.
33. Andersson, L., P. Boström, …, S. O. Olofsson. 2006. PLD1 and ERK2 regulate cytosolic lipid droplet formation. *J. Cell Sci.* 119:2246–2257.
34. Adeyo, O., P. J. Horn, …, J. M. Goodman. 2011. The yeast lipin orthologue Pah1p is important for biogenesis of lipid droplets. *J. Cell Biol.* 192:1043–1055.
35. Chen, X., and J. M. Goodman. 2017. The collaborative work of droplet assembly. *Biochim. Biophys. Acta.* 1862 (10 Pt B):1205–1211.

36. Mishra, S., R. Khaddaj, …, R. Schneiter. 2016. Mature lipid droplets are accessible to ER luminal proteins. *J. Cell Sci.* 129:3803–3815.

37. Ohsaki, Y., J. Cheng, …, T. Fujimoto. 2008. Lipid droplets are arrested in the ER membrane by tight binding of lipidated apolipoprotein B-100. *J. Cell Sci.* 121:2415–2422.

38. Thiam, A. R., and M. Beller. 2017. The why, when and how of lipid droplet diversity. *J. Cell Sci.* 130:315–324.

39. Paul, D., V. Madan, and R. Bartenschlager. 2014. Hepatitis C virus RNA replication and assembly: living on the fat of the land. *Cell Host Microbe*. 16:569–579.

40. Sturley, S. L., and M. M. Hussain. 2012. Lipid droplet formation on opposing sides of the endoplasmic reticulum. *J. Lipid Res.* 53:1800–1810.

41. Beller, M., C. Sztalryd, …, B. Oliver. 2008. COPI complex is a regulator of lipid homeostasis. *PLoS Biol.* 6:e292.

Biophysical Journal, Volume *114*

Supplemental Information

An Asymmetry in Monolayer Tension Regulates Lipid Droplet Budding Direction

Aymeric Chorlay and Abdou Rachid Thiam

A Tension Asymmetry Between Monolayers Regulates the Budding Direction of Reconstituted Lipid Droplets

Aymeric Chorlay[1], Abdou Rachid Thiam[1,*]

[1] Laboratoire de Physique Statistique, Ecole Normale Supérieure, PSL Research University, Sorbonne Université, UPMC Université Paris 06, Université Paris Diderot, CNRS, Paris, France

Supporting Material

Figures S1

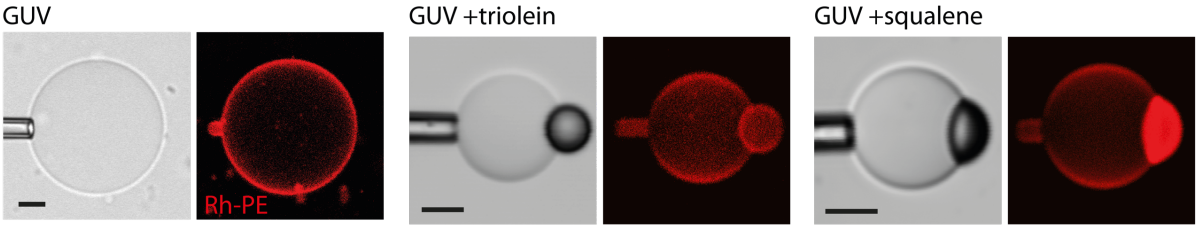

Supplementary Figure S1 | Illustration of micro-aspiration measurement of the bilayer surface tension of PC GUV, PC GUV embedded with a triolein LD and PC GUV embedded with squalene LD. Scale bar is 10 µm.

Figures S2

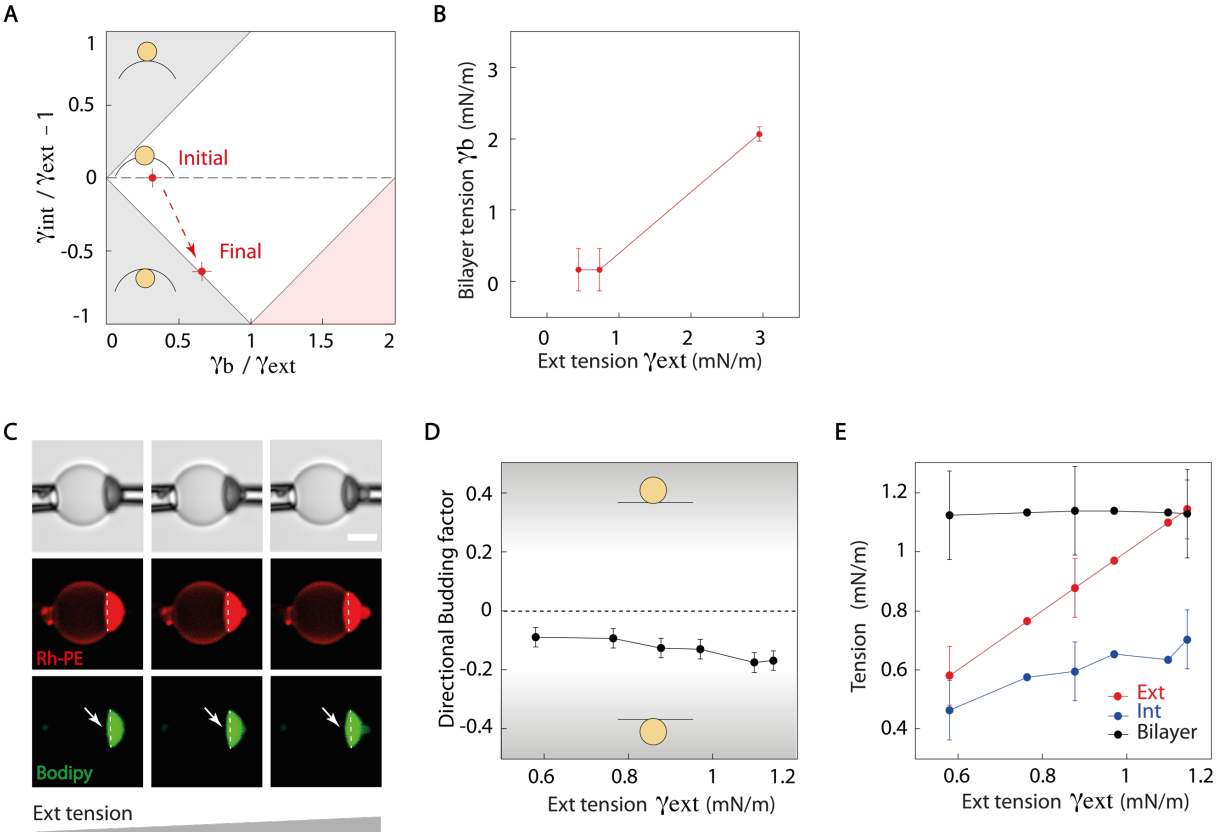

Supplementary Figure S2 | A) Initial and final states of the LD shape from the Fig. 4A, indicated on the phase diagram of Fig.3A. **B**) Bilayer tension corresponding to the experiment shown in Fig. 4A, calculated using the technique describe in supplementary text 2 **C)** Squalene LD embedded in a GUV.

External monolayer tension in increased with right micropipette and bilayer tension is kept constant with the left micropipette. The LD tends to internalized (arrow). Scale bar is 10 µm. **D)** Corresponding Directional budding factor as a function of the external tension. **E)** Evolution of the three tensions as the external tension is increased. Bilayer tension is kept constant.

Figures S3

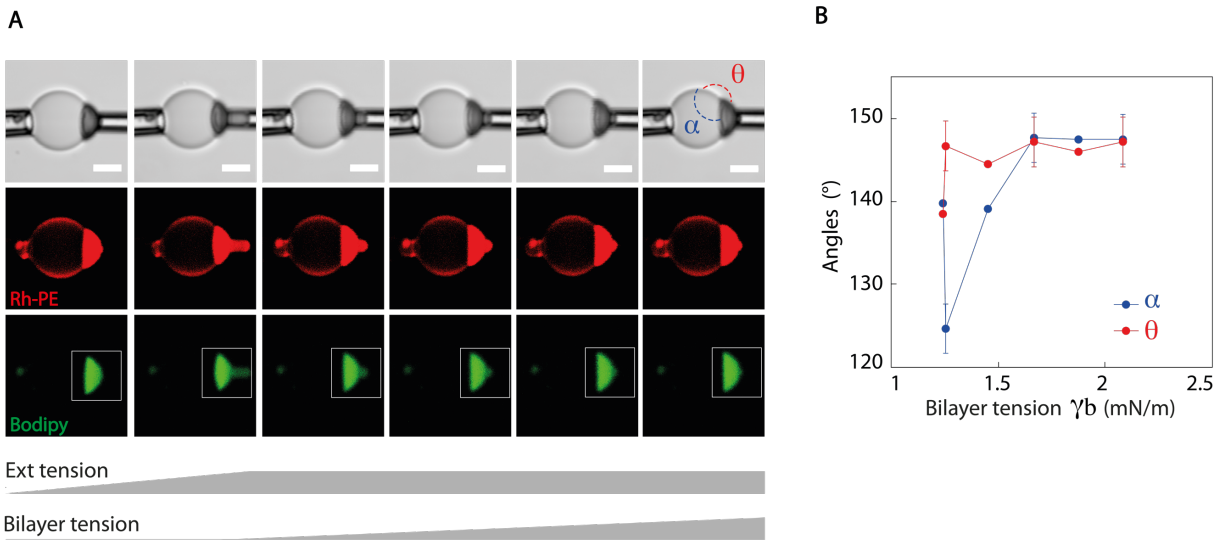

Supplementary Figure S3 | A) Full frame view of the experiment shown in (Fig. 5A). Scale bar is 10 µm **B)** Corresponding angles alpha and theta plotted as a function of the bilayer tension.

Figures S4

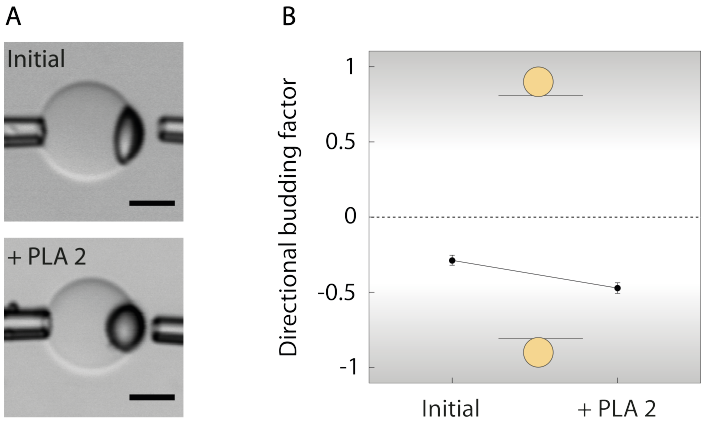

Supplementary Figure S4 | A) PLA2 enzyme is added to the external medium of a PC/PA (70/30) GUV embedding a triolein LD. (PA: dioleoylphosphatidic acid**)** PA was added to increase the bilayer tension and obtain droplets that were not readily budded, which often occurred with pure PC. The evolution of the droplet is observed over time. Scale bar is 10 µm. **B)** Decreasing directional budding factor showing a asymetrization of the LD position.

Supplementary text 1 | Determination of the shape and position of an LD in a GUV bilayer.

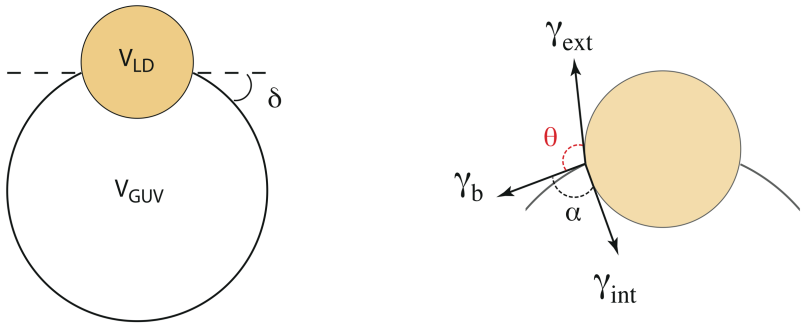

Considering that the lipid droplet's shape is driven by the equilibrium of the three surface tensions (bilayer γ_b, external monolayer γ_{ext} and internal monolayer γ_{int}) (Eq. 1), can be projected on the bilayer axis and lead to (Eq. 2).

$$\overrightarrow{\gamma_b} + \overrightarrow{\gamma_{int}} + \overrightarrow{\gamma_{ext}} = \vec{0} \qquad (1)$$

$$\begin{aligned} \gamma_b &= -\gamma_{int}\cos(\alpha) - \gamma_{ext}\cos(\theta) \\ \gamma_{ext}\sin(\theta) &= \gamma_{int}\sin(\alpha) \end{aligned} \qquad (2)$$

Moreover, the conserved volume of the LD and the GUV gives two other equations (Eq. 3,4):

$$V_{LD} = \frac{4\,\Pi Ro^3}{3}\left(\frac{2-\cos(\theta-\delta)^3+3\cos(\theta-\delta)}{\sin(\theta-\delta)^3} + \frac{2-\cos(\alpha-\delta)^3+3\cos(\alpha-\delta)}{\sin(\alpha-\delta)^3}\right) \qquad (3)$$

$$V_{GUV} = \frac{4\,\Pi Ro^3}{3}\left(\frac{2-\cos(\delta)^3+3\cos(\delta)}{\sin(\delta)^3} - \frac{2-\cos(\alpha-\delta)^3+3\cos(\alpha-\delta)}{\sin(\alpha-\delta)^3}\right) \qquad (4)$$

In order to determine the shape of the droplet, we only need three parameters: alpha, theta and delta, as a function of the tensions γ_b, γ_{int} and γ_{ext}.

Rearranging these equations leads to a set of 3 equations (Eq. 5,6,7) that can be solved numerically. The following equations (5, 6) Gives alpha and theta:

$$\cos(\theta) = \frac{{\gamma_{int}}^2 - {\gamma_{ext}}^2 - {\gamma_b}^2}{2\,\gamma_b\,\gamma_{ext}} \qquad (5)$$

$$\cos(\alpha) = \frac{{\gamma_{ext}}^2 - {\gamma_{int}}^2 - {\gamma_b}^2}{2\,\gamma_b\,\gamma_{int}} \qquad (6)$$

The last parameter delta is determined numerically, keeping the volumes constant (Eq. 7):

$$\frac{V_{LD}}{V_{GUV}} = \frac{\frac{2-\cos(\theta-\delta)^3+3\cos(\theta-\delta)}{\sin(\theta-\delta)^3} + \frac{2-\cos(\alpha-\delta)^3+3\cos(\alpha-\delta)}{\sin(\alpha-\delta)^3}}{\frac{2-\cos(\delta)^3+3\cos(\delta)}{\sin(\delta)^3} - \frac{2-\cos(\alpha-\delta)^3+3\cos(\alpha-\delta)}{\sin(\alpha-\delta)^3}} \qquad (7)$$

The profiles of the embedded LDs displayed in (Fig. 4B) are obtained using this mathematical model.

Supplementary text 2 | Determination of surface tensions.

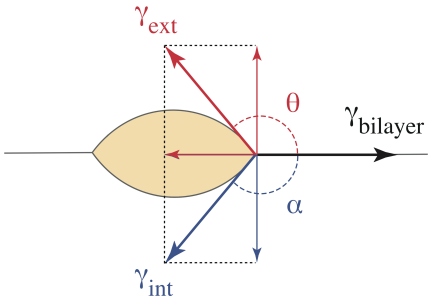

Given that the LD shape is driven by surface tension, the following equation describes the link between the bilayer tension γ_b, the external tension γ_{ext}, and the internal tension γ_{int}:

$$\gamma_b = -\gamma_{int}\cos(\alpha) - \gamma_{ext}\cos(\theta) \quad (1)$$

$$\gamma_{ext}\sin(\theta) = \gamma_{int}\sin(\alpha) \quad (2)$$

Measuring one of the tensions and the two angles (θ and α) allows us to determine the two other tensions using the two former equations. For example, knowing alpha, theta, and the external tension enable the determination of the bilayer tension by $\gamma_b = -(\gamma_{ext}\mathrm{cotan}(\alpha)\sin(\theta) + \cos(\theta))$, and γ_{int} through equation (2).